THE THEORY OF DISPERSAL DURING LAMINAR FLOW IN TUBES. II

By J. R. PHILIP*

[*Manuscript received March* 7, 1963]

Summary

The solution of the problem introduced in Part I is found for the case of large diffusion Péclet number (Υ). The work is carried out principally in the third approximation of the Galerkin method, and the results are presented in some detail.

The degree of the polynomial equation in the eigenvalues is halved by proceeding to the limit as $\Upsilon \to \infty$. The roots retained are found to be just those roots which are physically admissible.

A comparison of results of the first three approximations suggests that the Galerkin method is rapidly convergent and that the third approximation is accurate enough for the present purpose.

Results obtained from the analysis include the dependence of the (generally complex) apparent longitudinal diffusivity on frequency; a criterion for the validity of the diffusion approximation; and (when input concentration is periodic with time) the wave velocity. The wave velocity always exceeds the mean flow velocity, high frequency waves travelling faster than low frequency ones.

I. INTRODUCTION

The present work follows on immediately from Part I (Philip 1963), and we carry over the symbolism from that paper. We begin by considering the first three approximations to the solution of the system (1.5.1), (1.5.2) of Part I, and the choice of the physically appropriate roots. The remainder of the paper is a detailed study of the solution in the case of large Péclet number.

II. THE FIRST THREE APPROXIMATIONS

As indicated in Section VI of Part I, we shall be working principally in the third approximation. In order to secure some insight into the rate of convergence of the Galerkin method (and into the accuracy of the third approximation), it is desirable to give some attention to the first and second approximations also.

To proceed as far as the third approximation we need the following numerical values:

$$\left.\begin{array}{lll} a_{01} = -\,1\cdot3529, & a_{10} = -\,0\cdot2195, & a_{20} = +0\cdot0488, \\ a_{02} = +\,0\cdot5416, & a_{12} = -\,0\cdot5751, & a_{21} = -0\cdot3193, \\ \lambda_1^2 = 14\cdot682, & \lambda_2^2 = 49\cdot218. & \end{array}\right\} \quad (2.2.1)$$

Except for a_{12} and a_{21}, all these were found simply with the aid of tables of $J_0(x)$ and of the roots of $J_1(x)$ (Watson 1944). The values of a_{12} and a_{21} were deduced from the result

$$\int_0^1 \rho^3\, J_0(\lambda_1\rho)\,.\,J_0(\lambda_2\rho)\,d\rho = -0\cdot025901 \pm 0\cdot000044,$$

* Division of Plant Industry, C.S.I.R.O., Canberra.

secured by the use of Simpson's formula with end correction (Lanczos 1957, p. 44) over twenty panels.

(a) *First Approximation*

The first approximation is, evidently,

$$\alpha^2/\Upsilon^2-\alpha-\Omega\mathrm{i} = 0, \tag{2.2.2}$$

the roots of which are

$$\tfrac{1}{2}\Upsilon^2\,[1\pm(1+4\Omega\mathrm{i}/\Upsilon^2)^{\frac{1}{2}}]. \tag{2.2.3}$$

Now for Ω and Υ both real, and $\Omega/\Upsilon^2 \neq 0$,

$$\mathscr{R}[(1+4\Omega\mathrm{i}/\Upsilon^2)^{\frac{1}{2}}] > 1. \tag{2.2.4}$$

The negative sign in (2.2.3) must therefore be taken if $\mathscr{R}[\alpha]$ is to be negative, as the physical problem demands. It follows that $(\alpha_0)_1$, the zeroth eigenvalue in the first approximation, is given by

$$(\alpha_0)_1 = \tfrac{1}{2}\Upsilon^2\,[1-(1+4\Omega\mathrm{i}/\Upsilon^2)^{\frac{1}{2}}]. \tag{2.2.5}$$

The results given in (2.2.6) follow simply from (2.2.5):

$$\frac{1}{D}\lim_{\Omega/\Upsilon^2\to 0} K_1 = 1,$$

$$\frac{1}{D}\lim_{\Omega/\Upsilon^2\to 0} \frac{K_1}{\Upsilon^2} = \Upsilon^{-2},$$

$$\frac{1}{D}\lim_{\Upsilon\to\infty}\left[\lim_{\Omega\to 0}\frac{K_1}{\Upsilon^2}\right] = 0. \tag{2.2.6}$$

Here we have written K_1 to denote the value of K deducible from (1.4.10) when $(\alpha_0)_1$ is substituted for α. It will be clear later that the first approximation is a poor one, and that the only use of these results is to provide information on the convergence of the Galerkin method.

(b) *Second and Third Approximations*

The second approximation is

$$\begin{vmatrix} \alpha^2/\Upsilon^2-(\alpha+\Omega\mathrm{i}) & a_{10}\alpha \\ a_{01}\alpha & \alpha^2/\Upsilon^2-(4\alpha/3+\lambda_1^2+\Omega\mathrm{i}) \end{vmatrix} = 0, \tag{2.2.7}$$

a quartic in α, of which only two roots, $(\alpha_0)_2$, $(\alpha_1)_2$, are physically admissible. Similarly the third approximation,

$$\begin{vmatrix} \alpha^2/\Upsilon^2-(\alpha+\Omega\mathrm{i}) & a_{10}\alpha & a_{20}\alpha \\ a_{01}\alpha & \alpha^2/\Upsilon^2-(4\alpha/3+\lambda_1^2+\Omega\mathrm{i}) & a_{21}\alpha \\ a_{02}\alpha & a_{12}\alpha & \alpha^2/\Upsilon^2-(4\alpha/3+\lambda_2^2+\Omega\mathrm{i}) \end{vmatrix} = 0, \tag{2.2.8}$$

is a sextic in α, of which only three roots, $(\alpha_0)_3$, $(\alpha_1)_3$, $(\alpha_2)_3$, are physically admissible.

(c) *The Selection of Physically Admissible Roots*

Reverting for the moment to (2.2.2), we observe that the two roots of this equation tend to the values

$$Y^2+\Omega \mathrm{i}, \qquad -\Omega^2/Y^2-\Omega \mathrm{i}, \tag{2.2.9}$$

as $\Omega/Y^2 \to 0$. The latter of (2.2.9) is the physically valid root, and it is seen that the acceptable root as $Y \to \infty$ ($\Omega \neq 0$) is retained when the operations of solving the equation and proceeding to the limit are reversed, that is,

$$\text{root of } [\lim_{Y\to\infty} (2.2.2)] \equiv \lim_{Y\to\infty} [\text{physically valid root of } (2.2.2)],\ \Omega \neq 0. \tag{2.2.10}$$

A relationship similar to (2.2.10) holds for both (2.2.7) and (2.2.8) as well. The establishment of a general theorem along these lines appears to be difficult. We observe, however, that it is a plausible conjecture that each equation of the form (1.6.4), considered as a quadratic in a, has one physically admissible root and one which is physically inadmissible. The condition for this to be so is that

$$\left| \mathscr{R}\left[\left(C_n^2+\frac{4(\lambda_n^2+\Omega \mathrm{i})}{Y^2}\right)^{\frac{1}{2}}\right] \right| > \left| \mathscr{R}[C_n] \right|$$

for all n, where

$$C_n = 2-(\sum_0^\infty B_m a_{mn})/B_n.$$

It follows that a more specific condition under which

$$\text{each root of } [\lim_{Y\to\infty} (1.6.7)] \equiv \lim_{Y\to\infty} [\text{a physically valid root of } (1.6.7)],$$
$$\Omega \neq 0, \tag{2.2.11}$$

is that

$$\mathscr{R}\left[\left(C_n^2+\frac{4(\lambda_n^2+\Omega \mathrm{i})}{Y^2}\right)^{\frac{1}{2}}\right] > \mathscr{R}[C_n] > 0. \tag{2.2.12}$$

(2.2.12) is apparently satisfied, but a proof has not been attempted.

(d) *Schema for Solving (2.2.7), (2.2.8), etc.*

Equations (2.2.7) and (2.2.8) are, respectively, quartic and sextic equations with coefficients which are complex and which are functions of Y and Ω. Clearly, we cannot expect to obtain the roots as explicit functions of Y and Ω; and, at first glance, the task of determining the whole set of roots for $0 < Y < \infty$ and $0 < \Omega < \infty$, and of discarding the physically inadmissible ones, seems a very heavy undertaking. However, with the aid of the preceding considerations on the admissibility of roots in the limit as $Y \to \infty$ ($\Omega \neq 0$), we may develop the following schema, which leads fairly readily to solutions for the whole Ω-range and a substantial part of the Y-range. The following account refers specifically to the third approximation, but the application to the second approximation (or to higher approximations) will be evident.

(i) Halve the degree of the equation by proceeding to the limit as $\Upsilon \to \infty$ ($\Omega \neq 0$). Thus (2.2.8) reduces to

$$\begin{vmatrix} -(\alpha+\Omega\mathrm{i}) & a_{10}\alpha & a_{20}\alpha \\ a_{01}\alpha & -(4\alpha/3+\lambda_1^2+\Omega\mathrm{i}) & a_{21}\alpha \\ a_{02}\alpha & a_{12}\alpha & -(4\alpha/3+\lambda_2^2+\Omega\mathrm{i}) \end{vmatrix} = 0, \qquad (2.2.13)$$

and the task of securing the roots reduces to the simpler problem of solving a cubic. The roots so obtained may be adopted not only for infinite Υ, but also for large Υ, where the meaning of "large" will be clarified later.

(ii) We suppose now that $(\alpha_{\Omega,\Upsilon,s})_3$ has been established for $\Upsilon = \infty$, $s = 0, 1, 2$. It is convenient to express these functions of Ω in the form $g_s(w)$, where

$$w = \mathrm{i}\Omega. \qquad (2.2.14)$$

We observe that, by replacing w (i.e. $\mathrm{i}\Omega$) in (2.2.13) by $(w-\alpha^2/\Upsilon^2)$, we recover (2.2.8). Further, it may be shown that the $g_s(w)$ (which we may suppose established along the imaginary axis) may be analytically continued, at least onto the relevant region of the complex plane. These two considerations lead to a means of deducing $(\alpha_{\Omega,\Upsilon,s})_3$ for Υ finite from $g_s(w)$. This process will be developed in Part III (Philip, in preparation).

III. The Second Approximation for Large Peclet Number

The second approximation for large Péclet number reduces to the quadratic

$$(4/3-a_{10}\,.\,a_{01})\alpha^2+(\lambda_1^2+7w/3)\alpha+(\lambda_1^2 w+w^2) = 0. \qquad (2.3.1)$$

The roots are

$$(\alpha_0)_2,\,(\alpha_1)_2 = -\frac{(14\cdot682+7w/3)\pm(215\cdot56+7\cdot648w+1\cdot2987w^2)^{\frac{1}{2}}}{2\cdot0728}. \qquad (2.3.2)$$

We have used numerical values (2.2.1) to secure (2.3.2). When $|w|$ is small, $(\alpha_0)_2$, $(\alpha_1)_2$ may be expanded in ascending powers of w. The leading terms are:

$$\left.\begin{aligned} (\alpha_0)_2 &= -w+0\cdot02022w^2, \\ (\alpha_1)_2 &= -14\cdot166-1\cdot2514w-0\cdot02022w^2. \end{aligned}\right\} \qquad (2.3.3)$$

When $|w|$ is large, expansions in descending powers of w may be made. The leading terms are:

$$\left.\begin{aligned} (\alpha_0)_2 &= -0\cdot5905w-5\cdot3985, \\ (\alpha_1)_2 &= -1\cdot6609w-8\cdot7679. \end{aligned}\right\} \qquad (2.3.4)$$

Clearly, K_2, the second approximation to K, may be deduced from (2.3.2). In particular, we may use (2.3.3) in (1.4.10) to obtain the result

$$\frac{1}{D}\lim_{\Upsilon\to\infty}\left(\lim_{\Omega\to 0}\frac{K_2}{\Upsilon^2}\right) = 0\cdot02022 = \frac{1}{49\cdot45}. \qquad (2.3.5)$$

The exact value of the numerical term in (2.3.5) is $64/\lambda_1^6$.

IV. The Third Approximation for Large Peclet Number

The numerical values (2.2.1) reduce (2.2.13) to the cubic

$$\alpha^3+(64\cdot5767+3\cdot62221w)\alpha^2+(664\cdot775+137\cdot164w+3\cdot37314w^2)\alpha$$
$$+(664\cdot775w+58\cdot7845w^2+0\cdot919946w^3) = 0. \tag{2.4.1}$$

(a) Solution for |w| Small

When $|w|$ is small, the roots of (2.4.1) may be found as expansions in ascending powers of w. It is useful to begin this process by obtaining the roots of (2.4.1) in the limit as $w \to 0$. These are simply found to be 0, $-12\cdot8522$, and $-51\cdot7244$. The expansions for $(\alpha_0)_3$, $(\alpha_1)_3$, and $(\alpha_2)_3$ may then be developed by a process of equating coefficients. (The author employed a form of "long division" with all coefficients of the remainder equated to zero.) The results of this process are:

$$(\alpha_0)_3 = g_0(w) = -w+0\cdot0207631w^2-0\cdot00050444w^3$$
$$-0\cdot0000085865w^4+0\cdot00000107368w^5+0\cdot0000000081319w^6, \tag{2.4.2}$$

$$(\alpha_1)_3 = g_1(w) = -12\cdot8522-1\cdot00036w-0\cdot005208w^2, \tag{2.4.3}$$

$$(\alpha_2)_3 = g_2(w) = -51\cdot7244-1\cdot62186w-0\cdot015554w^2. \tag{2.4.4}$$

The expansion for $g_0(w)$ was taken further than those for the higher eigenvalues, since it is needed to greater accuracy in later work.

(2.4.2), combined with (1.4.10), yields an expansion for K_3 for large Péclet number and small $|w|$. This is

$$K_3/D = Y^2(0\cdot0207361+0\cdot0003577w-0\cdot000078709w^2). \tag{2.4.5}$$

It follows that

$$\frac{1}{D}\cdot\lim_{Y\to\infty}\left(\lim_{\Omega\to\infty}\frac{K_3}{Y^2}\right) = 0\cdot0207361 = \frac{1}{48\cdot16}. \tag{2.4.6}$$

(b) Solution for |w| Large

When $|w|$ is large, it is useful to rewrite (2.4.1) as

$$\alpha_*^3+(3\cdot6221+64\cdot5767w_*)\alpha_*^2+(3\cdot37314+137\cdot164w_*+664\cdot775w_*^2)\alpha_*$$
$$+(0\cdot919946+58\cdot7845w_*+664\cdot775w_*^2) = 0. \tag{2.4.7}$$

Here we have put

$$\alpha_* = \alpha/w, \qquad w_* = w^{-1}. \tag{2.4.8}$$

We may then again employ the procedure described immediately above to secure expansions for $(\alpha_0)_3/w$, $(\alpha_1)_3/w$, $(\alpha_2)_3/w$ in terms of w_*. The results may be rearranged as expansions in descending powers of w, which are valid for $|w|$ large:

$$(\alpha_0)_3 = g_0(w) = -0\cdot5321w-11\cdot1026+531\cdot316w^{-1}-31{,}741w^{-2}$$
$$+1{,}023{,}230w^{-3}-52{,}893{,}300w^{-4}\ \ldots, \tag{2.4.9}$$

$$(a_1)_3 = g_1(w) = -0\cdot7337w - 21\cdot674 - 768\cdot72w^{-1} + 66{,}882w^{-2} \ldots, \quad (2.4.10)$$

$$(a_2)_3 = g_2(w) = -2\cdot3564w - 23\cdot278 \ldots. \quad (2.4.11)$$

Here, also, the expansion for $g_0(w)$ was taken further than those for the higher eigenvalues, because of the later need to know $g_0(w)$ accurately.

(c) *Solution for 10 $\leqslant |w| \leqslant$ 100*

No formal study of the convergence of the expansions for $|w|$ small and large has been made. Comparison with results obtained independently for particular numerical values of w suggest that the expansions for $|w|$ small may be used for $|w| < 10$, and that the expansions for $|w|$ large may be used for $|w| > 100$.

For intermediate $|w|$, we may develop expansions about $w = w_0$, where w_0 is a pure imaginary value of w, such that $10 < -iw_0 < 100$, for which we have directly solved the cubic (2.4.1) (by the method indicated below). Such expansions may be

TABLE 1

VALUES OF $g_0(w)$, $g_1(w)$, $g_2(w)$ ESTABLISHED BY DIRECT SOLUTION OF (2.4.1)

w	$g_0(w)$	$g_1(w)$	$g_2(w)$
10 i	−2·15− 9·36i	−12·31−10·06i	−50·12−16·30i
15 i	−4·31−12·21i	−12·33−17·45i	−47·93−24·68i
17·5i	−4·89−13·14i		
20 i	−5·20−14·15i	−14·87−24·74i	−44·51−33·55i
25 i	−5·51−16·45i	−19·60−30·02i	−39·47−44·08i
35 i	−5·85−21·64i		
50 i	−6·32−29·74i	−25·75−40·23i	−32·51−111·13i
70 i	−7·03−40·71i		
100 i	−8·22−56·88i	−24·44−72·88i	−31·92−232·46i

developed by the methods of subsections (*a*) and (*b*) above, (*a*) being the natural choice, at least for the smaller values of $|w_0|$. Expansions of type (*b*) are possibly more useful for large values of $|w_0|$. The advantage of all such expansions about w_0 is that their continuation onto the complex plane, which we shall require in Part III, may be undertaken without loss of accuracy.

In the present work, we have proceeded in a less satisfactory, but far less laborious, way. We have found directly solutions of (2.4.1) by iterative use of the "rule of false position". (The fact that the roots are complex makes the calculation somewhat awkward, but prudent choice of the initial estimate of $g_0(w)$ by reference to the expansions for $|w|$ small and large, and to roots already determined directly for other values of w, greatly diminishes the labour. With $g_0(w)$ known, (2.4.1) reduces to a quadratic and $g_1(w)$, $g_2(w)$ follow at once.) The values of $g_0(w)$, $g_1(w)$, $g_2(w)$ established in this way are presented in Table 1.

We have then used results from Table 1 to secure the following power series approximations to $g_0(w)$:

$$10 \leqslant |w| \leqslant 25,$$
$$g_0(w) = (8\cdot 74+4\cdot 15\mathrm{i})-(2\cdot 1257-1\cdot 6650\mathrm{i})w -(0\cdot 0668+0\cdot 0944\mathrm{i})w^2+(0\cdot 001693-0\cdot 000920\mathrm{i})w^3; \quad (2.4.12)$$

$$25 \leqslant |w| \leqslant 100,$$
$$g_0(w) = -(4\cdot 77+4\cdot 29\mathrm{i})-(0\cdot 45442-0\cdot 28485\mathrm{i})w +(0\cdot 00004097+0\cdot 001469\mathrm{i})w^2 -(0\cdot 000007541+0\cdot 000001925\mathrm{i})w^3. \quad (2.4.13)$$

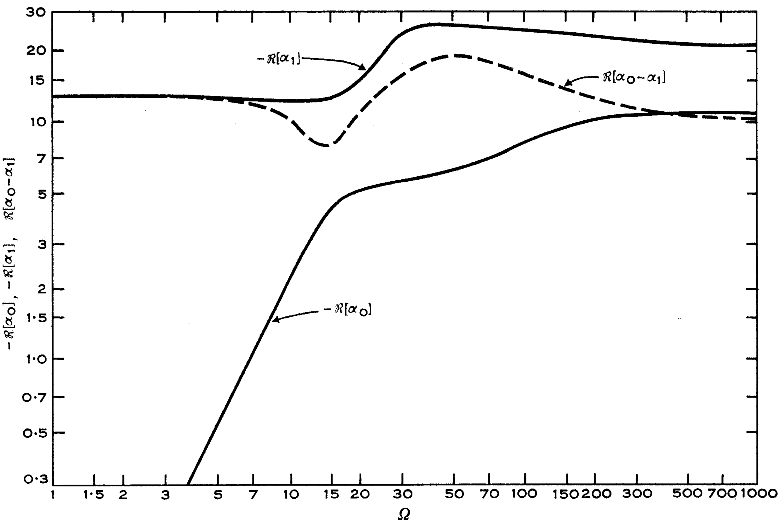

Fig. 1.—Logarithmic plot of the real parts of eigenvalues α_0, α_1 against reduced frequency Ω, in the third approximation. Broken curve represents $\mathscr{R}[\alpha_0-\alpha_1]$, which enters criterion (2.6.1).

These approximations are, strictly, valid only for interpolation along the positive imaginary axis of w. In Part III, however, we shall use these in regions of the complex plane not too far from the positive imaginary axis, where they may be expected to provide a simple means of continuation of sufficient accuracy.

(d) *Presentation of Solution in the Third Approximation*

It is convenient to bring together these various results and to present them graphically. Since it will be understood that we are treating the third approximation, we shall drop the suffix 3 from the α's for typographical simplicity. Figure 1 gives logarithmic plots of $\mathscr{R}[\alpha_0]$ and $\mathscr{R}[\alpha_1]$ against Ω. (It will be noted that $(\alpha_2)_3$ seems unlikely to be a good estimate of α_2, and we therefore omit it from the various figures.) Figure 2 gives, similarly, the plots of $\mathscr{I}[\alpha_0]$ and $\mathscr{I}[\alpha_1]$ against Ω.

The corresponding plots of α_0 and α_1 on the complex plane are given in Figure 3.

The dependence of K on Ω is most conveniently represented in terms of the quantity κ_3, defined as

$$\kappa_3 = \frac{1}{D} \lim_{Y\to\infty} \frac{K_3}{Y^2}. \tag{2.4.14}$$

Figure 4 gives the plot of κ_3 on the complex plane. This figure also shows the plot of $\kappa = \frac{1}{D} \lim_{Y\to\infty} \frac{K}{Y^2}$ according to the approximate analysis of Philip (1963). Figure 4

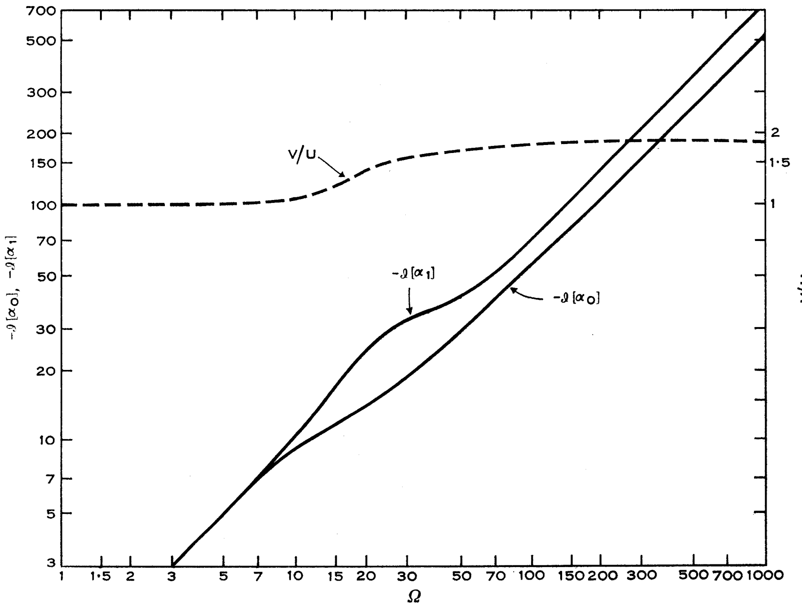

Fig. 2.—Logarithmic plot of the imaginary parts of eigenvalues α_0, α_1, against reduced frequency Ω, in the third approximation. Broken curve represents wave velocity in the form V/U. Note that scale for V/U is to right of figure.

also indicates the Taylor-Aris result, $\kappa = 1/48$, which is, evidently, the exact value of $\lim_{\Omega\to 0} \kappa$.

V. Rate of Convergence of the Galerkin Method

It is useful to employ as a parameter indicating the rate of convergence of the Galerkin method, as applied to the present problem, the quantity

$$\kappa_q(0) = \frac{1}{D} \lim_{\Omega\to 0} \left(\lim_{Y\to\infty} \frac{K_q}{Y^2} \right). \tag{2.5.1}$$

This quantity has the advantage that, from the analysis of Aris(1956), we have the result

$$\kappa_\infty(0) = 1/48, \tag{2.5.2}$$

which provides an exact standard for comparison with the various approximations.

Figure 5 shows the plot of $\kappa_q(0)$ against q. It is clear that $\kappa_q(0)$ converges very rapidly to $\kappa_\infty(0)$ as q increases; and it appears that the third approximation will provide results of sufficient accuracy for the purposes of the present investigation.

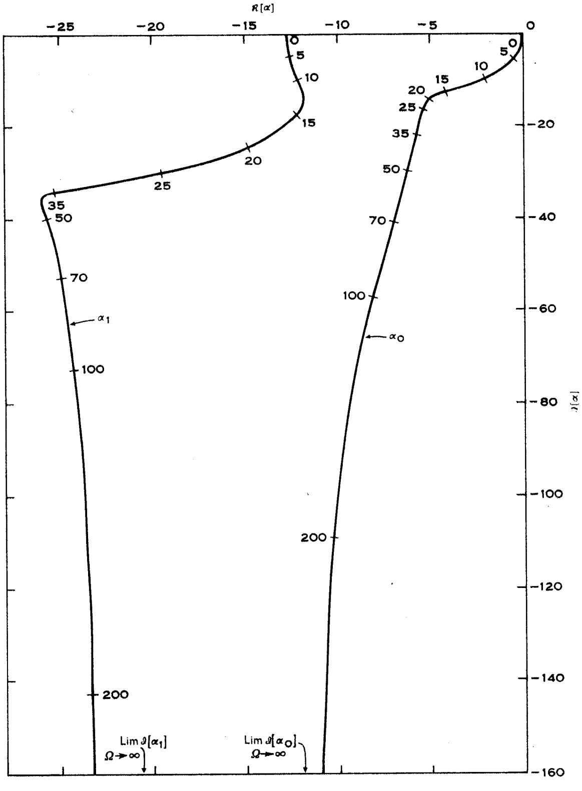

Fig. 3.—Plot of eigenvalues α_0, α_1 on the complex plane in the third approximation. Numbers along each curve denote values of reduced frequency Ω. Note that scale of real axis is four times that of imaginary axis.

VI. Validity of the Diffusion Approximation

In Part I, the criterion governing the minimum distance along the tube at which the diffusion approximation may be taken as valid, L, was established as

$$\frac{L}{a} \gg \frac{Y}{\mathscr{R}[\alpha_0 - \alpha_1]}. \tag{2.6.1}$$

[also (1.5.1)]

The quantity $\mathscr{R}[\alpha_0 - \alpha_1]$ has been plotted on Figure 1. It will be observed that this quantity varies mildly with Ω, but it is, essentially, of order of magnitude 10 throughout the range of Ω. It is therefore clear that a simple and useful criterion is

$$L/a \gg Y/10. \tag{2.6.2}$$

It is of some interest to compare this criterion with those of Taylor and Aris (cf. (1.3.2), (1.3.3), (1.3.8)). We note, in particular, that direct comparison with the Aris criterion (with numerical value 15 in place of the present 10) is confused by the different modes of introduction of length L. In any case, we have the result

$$\lim_{\Omega\to 0}\mathscr{R}[a_0-a_1] = 12\cdot 85, \tag{2.6.3}$$

and it is, strictly, the quantity 12·85 which should be used in any comparison with the 15 of Aris and with the various numerical coefficients proposed by Taylor.

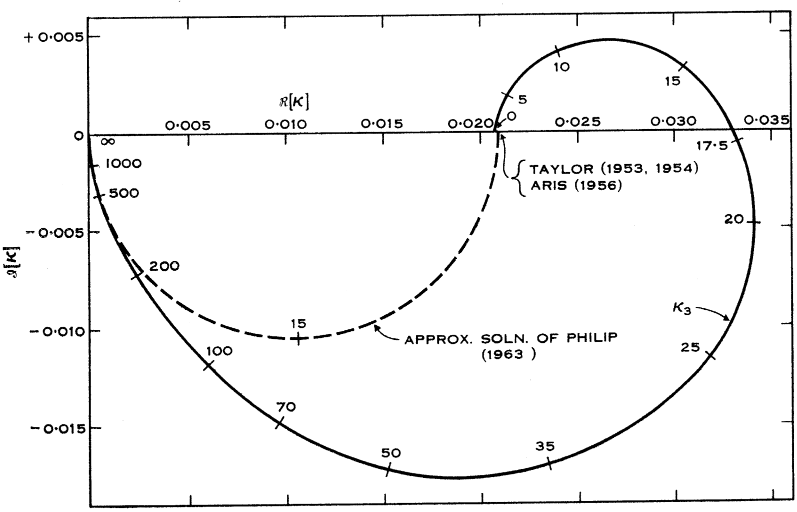

Fig. 4.—Full curve represents plot of apparent diffusivity, in form $\kappa = K/DY^2$, in the third approximation. Broken curve represents plot of κ according to approximate analysis of Philip (1963). Also shown is the result of Taylor (1953, 1954) and Aris (1956). Numbers along curves denote values of reduced frequency Ω.

VII. Wave Velocity

When the input concentration is a stationary random function of time, the concepts of wave velocity and phase shift are not meaningful. In the special case where input concentration is a periodic function of time, however, these concepts are valid. We discuss the matter here in terms of wave velocity only. A treatment in terms of phase shift is, of course, equally possible.

The "fundamental" wave of mean concentration c, associated with an input of reduced frequency Ω, is [cf. (1.4.8), (1.4.12)]

$$c = c_0 \exp[\Omega i\tau + a_0\xi/Y]. \tag{2.7.1}$$

The wave velocity, in the reduced space-time of ξ, τ, is seen to be

$$-\Omega Y/\mathscr{I}(a_0). \tag{2.7.2}$$

It follows from (1.2.3) that, in the space-time of x, t, the wave velocity V is given by

$$V/U = -\Omega/\mathscr{I}(\alpha_0). \tag{2.7.3}$$

The graph of V/U against Ω is given in Figure 2. It will be observed that V/U increases monotonically with Ω from the value 1 in the limit as $\Omega \to 0$ to the value $1 \cdot 879$ in the limit as $\Omega \to \infty$. We note the following expressions for V/U, which are valid, respectively, for small and large Ω.

$$V/U = (1-0 \cdot 000504\Omega^2)^{-1}, \tag{2.7.4}$$

$$V/U = 1 \cdot 879(1+999\Omega^{-2})^{-1}. \tag{2.7.5}$$

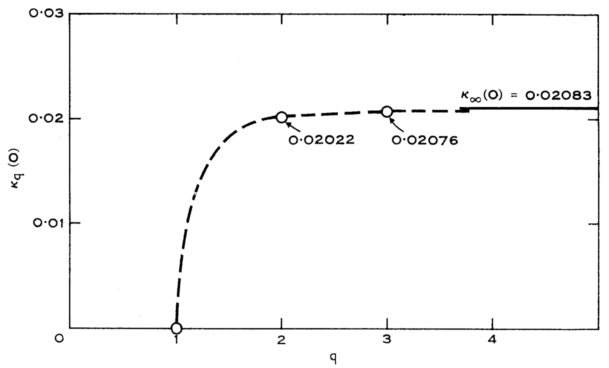

Fig. 5.—Plot of $\kappa_q(0)$ against q. $\kappa_q(0)$ represents the value of $\kappa(0)$ given by the qth approximation of Galerkin method. $\kappa_\infty(0)$ represents the exact value.

It will be seen that V exceeds U for all $\Omega > 0$. That is, the wave always travels down the tube more rapidly than the mean flow. We observe, further, that high frequency waves travel faster than low frequency ones.

VIII. Acknowledgment

The author gratefully acknowledges the helpfulness of discussions with Professor John W. Miles, Australian National University.

IX. References

Aris, R. (1956).—*Proc. Roy. Soc.* A **235**: 67.

Lanczos, C. (1957).—"Applied Analysis." (Pitman: London.)

Philip, J. R. (1963).—*Aust. J. Phys.* **16**: 287.

Taylor, Sir Geoffrey (1953).—*Proc. Roy. Soc.* A **219**: 186.

Taylor, Sir Geoffrey (1954).—*Proc. Roy. Soc.* A **225**: 473.

Watson, G. N. (1944).—"A Treatise on the Theory of Bessel Functions." 2nd Ed. (Cambridge Univ. Press.)